20th IMEKO TC4 International Symposium and
18th International Workshop on ADC Modelling and Testing
Research on Electric and Electronic Measurement for the Economic Upturn
Benevento, Italy, September 15-17, 2014

RF ranging based on space diversity techniques and directive antennas

V. Pasku, M.L. Fravolini, A. Moschitta

University of Perugia, Department of Engineering, Via G. Duranti, 93 06125 Perugia, Italy e-mail: valterpasku@libero.it, {antonio.moschitta,mario.fravolini}@unipg.it.

***Abstract* – In this paper, a ranging technique based on narrowband transmissions in the 2.4 GHz ISM band is discussed. Multipath mitigation techniques based on Multiple Input Multiple Output (MIMO) philosophy are considered, discussing the effect of antenna directivity on the achievable performance.**

I. INTRODUCTION

Indoor positioning techniques are subject of various research activities, since they are application enablers in various fields, including domotics, assisted navigation of commercial buildings of hospitals, and production line logistic.

Various solutions have been proposed, often based on ranging of bearing techniques of a mobile node with respect to a set of fixed beacons, followed by triangulation algorithms. In turn, ranging is obtained by transmitting a given signal with known parameters, whose propagation model is known and can be inverted after the received signal is collected. To this aim, the use of various kinds of signals is mentioned in the literature, including wideband or narrowband RF waves, low frequency inductively coupled EM signals, and ultrasounds [1]-[13]. The measured parameters can be the direction of arrival, the time of arrival, or the received signal strength.

Each of the mentioned approaches realizes a specific tradeoff, among various features, that include power consumption, implementation cost, and measurement accuracy. For instance, systems based of Ultra Wide Band signals tend to be accurate and robust to multipath, at a price of high power consumption and are implemented using expensive components. Similarly, systems based on inductively coupled low frequency EM fields are robust to multipath and penetrate through walls, but their performance can be reduced in presence of metallic masses, and have high power consumptions. Ultrasound solutions are usually accurate and cost effective, but suffer of a limited range and require Line of Sight (LOS) propagation.

In this paper, a technique based on narrowband RF transmissions is discussed, that can be implemented using low cost commercial transceivers, operating in the 2.4 GHz Industrial Scientific Medical (ISM) band. Narrowband RF signals are usually affected by multipath phenomena, especially in indoor environments, that, for Received Signal Strength (RSS) measurements, can lead to large ranging errors. On the other hand, 2.4 GHz ISM transmissions are well standardized, for instance in [5], and usually implemented in low cost low power transceivers, and the same hardware can be simultaneously used to perform range measurements and for communication purposes.

In a previous activity, the authors proposed a ranging system based MIMO philosophy, where the mobile node is equipped with a set of RF transceivers, with a spacing close to a wavelength [4]. In particular, it was shown that the proposed approach can effectively mitigate multipath effects, since multipath phenomena are unlikely to simultaneously affect all the mobile node transceivers, leading to a maximum ranging error of a few tens of centimeters. In this paper, the analysis is extended. In particular, the effect of antenna directivity is considered, assessing its effects on the proposed algorithms, and keeping into accounts rotations of the mobile node. The results obtained by the new model are compared with those obtained using an isotropic radiator.

II. SIMULATION MODEL AND RANGING ALGORITHMS

The considered simulation model extends that of [4] by keeping into account a realistic antenna radiation pattern. In particular, we assume that a fixed beacon is located in a known position, and that the mobile node is equipped with a set of 4 transceivers, arranged in a tetrahedral configuration [4]. Each transceiver collects a RSS measurement, and the 4 collected values can be combined according to various strategies [4]. The RF signal propagation has been analyzed in [4] using a ray tracing model, that is described in the following for the sake of clarity and extended by including the effect of antennas' radiation pattern. The algorithms adopted to refine the received power measurements are also described.

A. Simulation Model

Let us assume that both the beacon and the mobile node transceivers are in a box shaped room, each of the six faces aligned to the Cartesian axes, and characterized by an individual reflection coefficient. A ray tracing model

ISBN-14: 978-92-990073-2-7

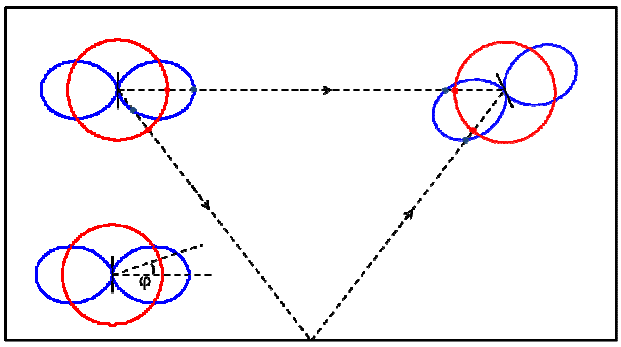

Fig. 1. Effects of directivity and antenna orientation on transmitting and receiving gain.

(optical) approximation can be used to describe RF propagation phenomena, assuming the typical size of a real room and the usage of frequencies in the GHz range. The ray tracing model is acceptable for propagation distances that exceed 3-4 wavelengths [4]. Assuming that the fixed beacon transmits to the mobile node a sinusoidal signal $s_{tx}(\cdot)$ with frequency f_0 and amplitude A_{tx}, the received signal $s(\cdot)$ for each transceiver of the mobile node can be expressed as

$$s_{tx}(t) = A_{tx}\sin(2\pi f_0 t)$$

$$s(t) = \sum_{i=0}^{6} s_i(t),$$

$$s_i(t) = \begin{cases} C_0 \sin\left(2\pi f_0\left(t - \dfrac{d_0}{c}\right)\right), & i = 0, \\ C_i \sin\left(2\pi f_0\left(t - \dfrac{d_i}{c}\right) + \varphi_i\right), & i = 1,\ldots,6 \end{cases} \quad (1)$$

$$C_0 = A_{tx} F(d_0) G_{Tx0} G_{Rx0},$$

$$C_i = A_{tx} F(d_i) |\Gamma_i| G_{Txi} G_{Rxi}, \quad i = 1,\ldots,6$$

$$\varphi_i = \angle\Gamma_i, \qquad F(d_i) = c/(4\pi f_0 d_i)$$

where d_0 is the length of LOS transmission path, Γ_i for $1 \le i \le 6$ is the reflection coefficient of the i-th wall, and d_i is the corresponding reflection path. The transmitting and receiving gains are considered respectively from G_{Txi} and G_{Rxi}. Eq. (1) is derived by assuming that only the single reflections can significantly influence the received signal, higher order reflections having negligible effects.

Eq (1) was used in [4] to simulate the received power measurements for a mobile node equipped with four transceivers, located in the vertexes of a regular tetrahedron, assuming isotropic antennas. Notice that, under such conditions, rotations of the mobile node are not expected to significantly affect the received power. However, (1) can be refined and made more realistic, by keeping into account antenna directivity. In particular, the transmitting and receiving antennas were modeled as quarter wavelength dipole radiators with gain G given by:

$$G(\varphi) = E \cdot D_{\max} \cdot \frac{RP}{\max(RP)}$$

$$RP = \left[\frac{\cos\left(\frac{\pi}{4}\cos\left(\frac{\pi}{2} - \varphi\right)\right) - \cos\left(\frac{\pi}{4}\right)}{\sin\left(\frac{\pi}{2} - \varphi\right)}\right]^2, \qquad D_{\max} = 1.53 \quad (2)$$

where φ is the angle between the direction of observation and the direction of the dipole axis, Fig. 1, D_{max} is the maximum directivity and E is the antenna efficiency assumed equal to 0.8.

Transmitting and receiving gain for the direct and reflected paths depend on the relative orientation between the dipole antennas, as shown in Fig. 1. It can be observed that, depending on the relative orientation between the two antennas, the received power of both the LOS signal and the reflected one can significantly change. Thus, (2) can be used with (1) to simulate more realistic scenarios, as shown in section III.

B. Correction Algorithms

Once RSS measurements have been collected, averaging techniques can mitigate the effects of multipath phenomena. Geometric averaging is preferable, since the arithmetic average can be dominated by the largest collected RSS value. Since the room dimensions are known, as additional information the maximum distance d_{max} that can occur between the fixed beacon and a mobile node is known. Using the free space propagation model, the received power P_{rxdBm} of the single transceiver expressed in dBm can be calculated as:

$$P_{rxdBm} = 10\log_{10}\left(G_{tx} G_{rx} \frac{A_{tx}^2}{2}\left(\frac{k_0}{d}\right)^2\right) + 30, \quad (3)$$

$$k_0 = \frac{\lambda}{4\pi}, \quad \lambda = \frac{c}{f_0}$$

where G_{tx} and G_{rx} are the transmitter and receiver antenna gain respectively, corresponding to the direct path, λ is the signal wavelength and c is the speed of light in vacuum. The knowledge of d_{max}, combined with Eq. (3) can be used to estimate $P_{min\ rxdBm}$, that is the minimum RSS expressed in dBm that would be measured under free space propagation conditions. Therefore, any measured power lower than $P_{min\ rxdBm}$ can be identified as a result of multipath and treated accordingly.

Assuming that the mobile node is equipped with N transceivers, a set of algorithms is described in the following, operating on the collected P_{rxdBm} measurements and providing a corrected received power estimation RSS_c. Since interference between received signal replicas can be both destructive and constructive, algorithms 0, 1 and 2 aim at mitigating the effect of fading from the destructive interference, and algorithms 3 and 4 also aim at mitigating the effects of constructive interference. The algorithms, presented in [4], are

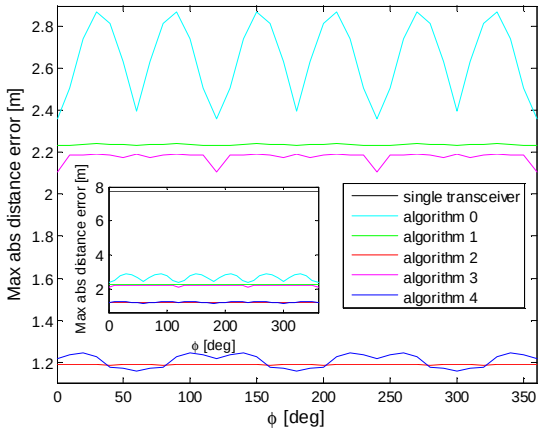

Fig. 2: Maximum ranging error, obtained for the considered MIMO based strategies, as a function of the azimuthal rotation, assuming isotropic radiators.

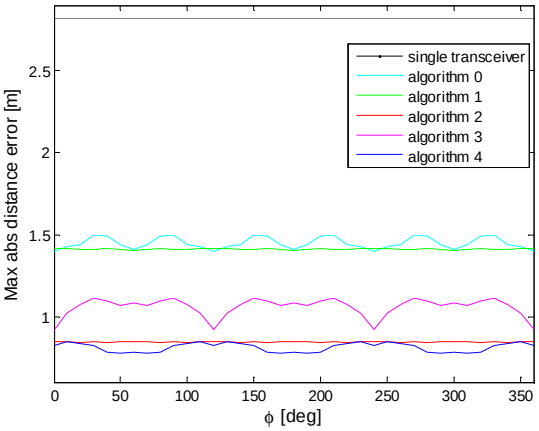

Fig. 3: Maximum ranging error, obtained for the considered MIMO based strategies, as a function of the azimuthal rotation, assuming directive radiators.

described here for the sake of clarity.

Algorithm 0: the corrected received power estimation RSS_c is obtained by averaging the received power measurements, expressed in dBm:

$$RSS_c = \frac{1}{N}\sum_{n=0}^{N-1} P_{rxdBm,n} \qquad (4)$$

where P_{rxdBm} is the power measured by the n-th transceiver equipping the mobile node.

Algorithm 1: the collected measurements are compared with the minimum received possible power under free space propagation conditions $P_{min\ dBm}$, discarding any result P_{rxdBm} such that $P_{rxdBm} < P_{min\ dBm}$. The remaining N_1 measurements such that $P_{rxdBm} \geq P_{min\ dBm}$ are averaged, according to

$$RSS_c = \begin{cases} \frac{1}{N_1}\sum_{n=0}^{N_1-1} P_{rxdBm,n}, & N_1 > 0 \\ P_{\min,dBm}, & N_1 = 0 \end{cases} \qquad (5)$$

If all the received power measurements are lower than $P_{min\ dBm}$ the maximum distance is assumed.

Algorithm 2: the collected received power measurements are preliminary corrected and then *Algorithm 0* is applied. The corrected power measurements P_{cdBm} are given by

$$P_{cdBm,n} = \max(P_{rxdBm,n}, P_{\min,dBm}), \quad n = 0,...,N-1 \qquad (6)$$

and then RSS_c is obtained by

$$RSS_c = \frac{1}{N}\sum_{n=0}^{N-1} P_{cdBm,n}\ . \qquad (7)$$

Algorithm 3: the maximum collected P_{rxdBm} value is supposed as a result of constructive interference and discarded; *Algorithm* 2 is applied to the remaining N-1 P_{rxdBm} values.

Algorithm 4: the preliminary correction (6) is applied on the collected power measurements and then RSS_c is obtained as the mean of the maximum and minimum corrected values:

$$\begin{aligned} RSS_c &= \frac{RSS_{\max} + RSS_{\min}}{2}, \\ RSS_{\max} &= \max(P_{cdBm,n}, \quad n = 0,...,N-1), \\ RSS_{\min} &= \min(P_{cdBm,n}, \quad n = 0,...,N-1), \end{aligned} \qquad (8)$$

The RSS_c values obtained with the previous algorithms can be used to estimate the distance d between the two nodes by inverting (3):

$$\hat{d} = \sqrt{\frac{P_{tx}G_{tx}G_{rx}k_0^{\,2}}{\hat{P}_{rx}}}, \hat{P}_{rx} = 10^{\frac{RSS_c - 30}{10}}, P_{tx} = \frac{A_{tx}^2}{2}. \qquad (9)$$

In a practical scenario, the true values of G_{tx} and G_{rx}, that depend on the relative orientation of transmitting and receiving antennas, are not known in advance. Thus, a preliminary analysis was run, for a uniform grid of positions assumed by the mobile node in the *xy* plane, estimating the mean value of such gains, subsequently used in the following performance analyses when applying (9).

III. ANALYSIS OF RESULTS

The ranging problem was analyzed by assuming a box shaped room with a height of 3 m, a depth of 6 m, and a width of 6 m, running Montecarlo simulations. In particular, we considered a mobile node comprising 4 transceivers, arranged in a tetrahedral configuration, spaced by 16 cm, a face being parallel to the *xy* plane. Moreover, we assumed that the mobile node, whose nominal position is the barycenter of the tetrahedron, takes a set of positions, uniformly distributed on a horizontal plane in the room, at a height of 1.5 m, collecting RSS measurements from a beacon, located in (0.8,3,1.5). The room floor was modeled as a perfectly reflective surface, the other walls were modeled as perfectly absorbing surfaces.

Fig. 2 shows the maximum ranging error, obtained by assuming, for each position, an azimuthal rotation of the mobile node, assuming isotropic antennas. For reference

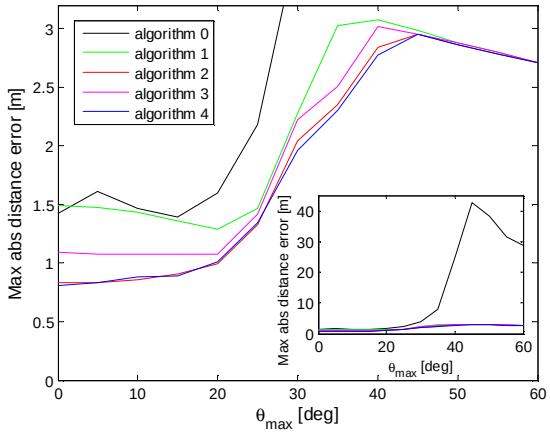

Fig. 4: maximum ranging error, as a function of the maximum elevation θ_{max}, obtained by assuming that the mobile node is equipped with 4 directive antennas, arranged in a tetrahedral configuration.

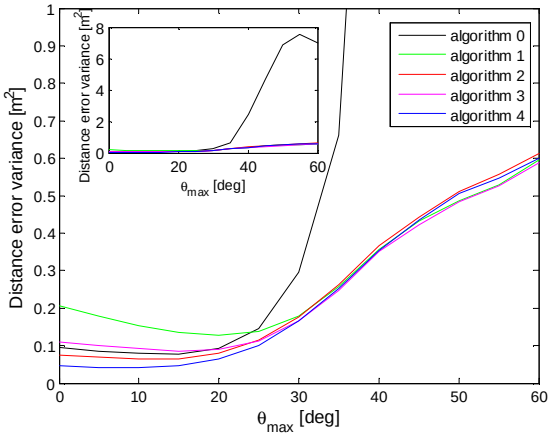

Fig. 5: ranging error variance, as a function of the maximum elevation θ_{max}, obtained by assuming that the mobile node is equipped with 4 directive antennas, arranged in a tetrahedral configuration

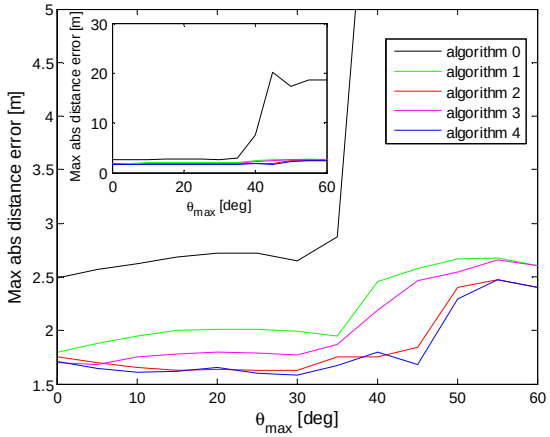

Fig. 6: maximum ranging error, as a function of the maximum elevation θ_{max}, obtained by assuming that the mobile node is equipped with 4 directive antennas, arranged in a tetrahedral configuration having different height with respect to the beacon.

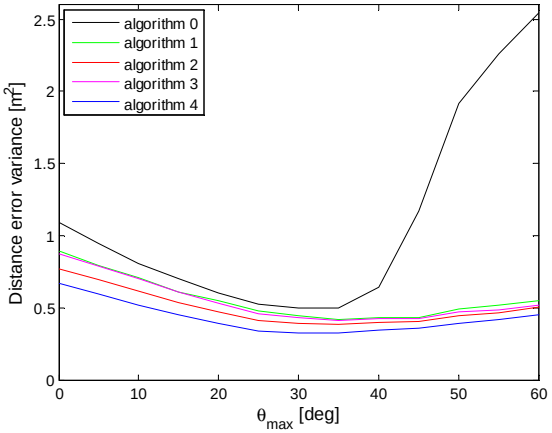

Fig. 7: ranging error variance, as a function of the maximum elevation θ_{max}, obtained by assuming that the mobile node is equipped with 4 directive antennas, arranged in a tetrahedral configuration having different height with respect to the beacon.

purposes, the performance obtained using a single transceiver mobile node is also shown, as a black curve in the inset of Fig. 2.

It can be observed that azimuthal rotations do not significantly affect the ranging performance, and that algorithm 4, together with algorithm 2, provides the best performance. Conversely, Fig 3 shows the maximum ranging error, this time obtained by assuming that the antennas are quarter wave dipoles. Once again, the maximum error is not significantly affected by azimuthal rotations, but the performance appears to be better than that obtained by assuming isotropic radiators. Such an improvement is explained by the antennas' directivity. In fact, since the beacon and the mobile node heights are very similar, the direct path received signal is amplified, while signal replicas received through reflective paths are attenuated (see Fig. 1). A similar behavior was observed for ranging error variance.

Then, the effect of elevation rotations was considered. This time, for each position in the considered horizontal plane, a random azimuth rotation ϕ and elevation θ were assumed for the tetrahedral mobile node with respect to its barycenter. The random rotation angles were uniformly distributed respectively in the interval [0, 2π] and [0, θ_{max}]. At first, simulations were run by assuming isotropic radiators, highlighting a negligible sensitivity of the ranging performance with respect to elevations rotation, both for the single transceiver and for the multiple transceiver approaches. Then, simulations were repeated, assuming to use directive antennas. Fig 4 shows the maximum ranging error, as a function of θ_{max}. The inset in Fig 4 shows the same data on a larger scale, to properly represent the black line, that describes the performance obtained using the less effective algorithm 0. As expected, the ranging error progressively increases with θ_{max}. Such a behavior can be explained by considering the radiation diagram of the considered

antennas. In fact, when a mobile antenna undergoes an elevation rotation, the direct path does no longer connect to the beacon antenna through the direction of maximum gain, emphasizing multipath phenomena. Moreover, using multiple transceivers seemingly reduces the ranging error by up to two orders of magnitude with respect to the single transceiver reference approach.

The analysis was the repeated for a set of positions, uniformly distributed on a horizontal plane at height 0.5m, that is at a different with respect to the beacon, once again located in (0.8, 3, 1.5). Figs 6 and 7 shows the maximum absolute ranging error and ranging error variance respectively. Algorithm 4 is again the best performing. A comparison with Figs 4 and 5 shows that the maximum distance error and error variance increase when the mobile node and the beacon are placed at different heights. On the other hand, the dynamic of maximum error and error variance in Figs 6 and 7 with respect to θ is smaller than that observed in Figs 4 and 5. Moreover, a performance worsening for θ_{max} exceeding a critical value can be observed both in Figs 4 and 5 and in Figs 6 and 7. In Figs 4 and 5, the critical value for θ_{max} is about 25°, while in Figs 6 and 7 it is about 35°. Such phenomenon can be ascribed to the lower gain of the direct path connecting the beacon and the mobile node when the transmitting and receiving antennas are not properly aligned. The different critical value in Figs 6 and 7 may be explained by observing that, due to the different heights of the beacon and the mobile node, in absence of rotations the transmitting and receiving antennas are not optimally aligned (see Fig. 1). Thus, a small random variation of θ may induce a better alignment, emphasizing the direct path with respect to multipath contributions. Thus, using transceivers at different heights may lead to a reduced performance, but also to a reduced sensitivity with respect to random rotations of the mobile node.

IV. CONCLUSIONS

A ranging technique based on RSS measurement, collected by a mobile node equipped with multiple transceivers, has been analyzed, keeping into account the effect of antennas' directivity. It is shown that, when the mobile node antennas are dipole-like and equally oriented, rotations about the dipole axis do not significantly affect the ranging error, while rotating the transceivers in different directions can significantly worsen the ranging performance, that is however more robust with respect to a single transceiver system. Usage of beacons and mobile nodes operating with suboptimal alignment has been investigated as well.

REFERENCES

[1] R. Mautz, "The challenges of indoor environments and specification on some alternative positioning systems," Proc. of 6th IEEE Workshop on Positioning, Navigation and Communication, WPNC 2009, pp. 29–36, DOI 10.1109/WPNC.2009.4907800.

[2] A. De Angelis, M. Dionigi, A. Moschitta, P. Carbone, "A Low-Cost Ultra-Wideband Indoor Ranging System," *IEEE Trans. on Instrumentation and Measurement*, Year 2009, Vol. 58 , No. 12, pp. 3935 – 3942, DOI 10.1109/TIM.2009.2020834.

[3] A.P. Sample, D.A. Meyer, J.R. Smith, "Analysis, Experimental Results, and Range Adaptation of Magnetically Coupled Resonators for Wireless Power Transfer," *IEEE Trans. on Industrial Electronics*, Vol. 58, No. 2, 2011, pp. 544-554.

[4] I. Neri, R. Centonze, M. L. Fravolini, A. Moschitta, "A simple ranging technique based on received signal strength measurements in a narrowband 2.4 GHz channel: a space diversity approach," IEEE M&N 2013, Naples, Italy, October 8-10 2013.

[5] D. Macii, A. Colombo, P. Pivato, D. Fontanelli, "A Data Fusion Technique for Wireless Ranging Performance Improvement," *IEEE Trans. on Instrumentation and Measurement*, , vol.62, no.1, pp.27,37, Jan. 2013.

[6] A. Colombo, D. Fontanelli, D. Macii, L. Palopoli, "Flexible Indoor Localization and Tracking Based on a Wearable Platform and Sensor Data Fusion," *IEEE Trans. on Instrumentation and Measurement*, , vol.63, no.4, pp.864,876, April 2014.

[7] Deng Zhongliang, Yu Yanpei, Yuan Xie, Wan Neng, Yang Lei, "Situation and development tendency of indoor positioning," *China Communications*, vol.10, no.3, pp.42,55, March 2013, doi: 10.1109/CC.2013.6488829.

[8] Chen Feng, Au W.S.A, S. Valaee, Zhenhui Tan, "Received-Signal-Strength-Based Indoor Positioning Using Compressive Sensing," IEEE Trans. on Mobile Computing, vol.11, no.12, pp.1983,1993, Dec. 2012, doi: 10.1109/TMC.2011.216.

[9] H. Hellmers, A. Norrdine, J. Blankenbach, A. Eichhorn, "An IMU/magnetometer-based Indoor positioning system using Kalman filtering," 2013 International Conference on Indoor Positioning and Indoor Navigation (IPIN 2013), pp.1,9, 28-31 Oct. 2013, doi: 10.1109/IPIN.2013.6817887.

[10] M. Dionigi, G. De Angelis, A. Moschitta, M. Mongiardo, P. Carbone, "A Simple Ranging System Based on Mutually Coupled Resonating Circuits," IEEE Trans. on Instrumentation and Measurement, vol.63, no.5, pp.1215,1223, May 2014, doi: 10.1109/TIM.2014.2298174.

[11] A. De Angelis, A. Moschitta, P. Carbone, M. Calderini, S. Neri, R. Borgna, M. Peppucci, "Design and characterization of an ultrasonic indoor positioning technique," Proc. of 2014 IEEE International Instrumentation and Measurement Technology Conference (I2MTC 2014), pp.1623,1628, 12-15 May 2014, doi: 10.1109/I2MTC.2014.6861020.

[12] A. Baniukevic, C.S. Jensen, Hua Lu, "Hybrid Indoor Positioning with Wi-Fi and Bluetooth: Architecture and Performance," 2013 IEEE 14th International Conference on Mobile Data Management (MDM 2013), vol.1, pp.207,216, 3-6 June 2013, doi: 10.1109/MDM.2013.30.

[13] IEEE standard 802.15.4